NJC

New Journal of Chemistry

A journal for new directions in chemistry

Accepted Manuscript

This article can be cited before page numbers have been issued, to do this please use: T. Boztepe, S. Scioli Montoto, M. E. Ruiz, V. Alvarez, G. R. Castro and I. Leon, *New J. Chem.*, 2020, DOI: 10.1039/D0NJ03940C.

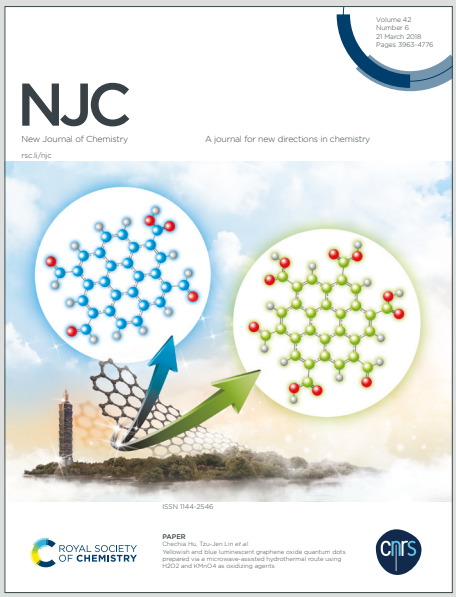

View Article Online
DOI: 10.1039/D0NJ03940C

ARTICLE

8-Hydroxyquinoline platinum(II) Loaded Nanostructured Lipid Carriers: Synthesis, Physicochemical Characterization and Evaluation of Antitumor Activity

Received 00th January 20xx,
Accepted 00th January 20xx

DOI: 10.1039/x0xx00000x

Boztepe T. [a], Scioli-Montoto S. [b], Ruiz M.E. [b], Alvarez V.A. [c], Castro G.R. [a], León I.E. [d] *

The incidence of cancer and the death rate increases every year in the world. The drug 8-hydroxyquinoline platinum(II) [PtCl(8-O-quinoline)(dmso)] (8HQ-Pt) has been identified as a promising antitumor complex. Nanostructured lipid carriers (NLC) are the second-generation drug nanocarrier systems that present superior advantages over other kinds of colloidal carrier systems. 8HQ-Pt compound loaded NLC formulations of cetyl esters (SS) were synthesized by ultrasonication in presence of two different liquid oils; capric triglyceride, or olive oil. The physicochemical and microscopic characterizations of NLC were analyzed by dynamic light scattering (DLS), transmission electron microscopy (TEM), fourier transformed infrared spectroscopy (FTIR), thermogravimetric analysis (TGA), differential scanning calorimetry (DSC) and X-ray diffraction analysis (XRD). In vitro drug release and cytotoxicity, cell uptake and apoptosis assays against the human colon cancer HT-29 were investigated. The results showed that NLCs indicated a narrow size distribution in the range of 136-159 nm mean particle diameter. The thermal characteristics analysis confirmed the stability of NLCs up to 185 °C. Encapsulation efficiencies of the 8HQ-Pt compound in NLCs were about 80% and 8HQ-Pt compound in the formulations showed controlled release profile during 72 h. The release profile of these two different formulations and the antitumor effect on HT-29 cell line were compared with the free 8HQ-Pt compound. The cellular uptake of two different NLC groups was proved by fluorescence microscopy and the presence of capric triglyceride liquid oil in the formulation increased the capacity of drug delivery to intracellularly when compared with olive oil.

Introduction

Cancer is the main cause of death worldwide, grew to 18.1 million novel cases and 9,6 million deaths in 2018. Lung, breast, colorectal, prostate and stomach cancers are leading types of cancer globally. Colorectal cancer (CRC) is the third of the most common cancers worldwide with approximately 1.8 million people diagnosed in 2018 and is ranked as the second leading cause of death (880.000 deaths in 2018) after lung cancer [1]. Genetic and lifestyle factors such as unhealthy nutrition, obesity, smoking, alcohol and lack of physical activity raise the risk of CRC [2].

Platinum-based metallodrugs have been used in the treatment of various solid tumors for decades, although they show a high level of toxicity and low bioavailability [3]. Cisplatin, carboplatin and oxaliplatin are well-known platinum(II) compounds that are anticancer drugs approved by the Food and Drug Administration (FDA, USA) for chemotherapy in the clinic [4]. Cisplatin is also called as cis-diamminedichloroplatinum(II) was used for bladder, testicular, ovarian, cervical, head, neck, colorectal and lung cancers [5,6]. Due to an active species of cisplatin, the drug is able to interact with purine nucleotide bases of DNA and induces DNA distortion, leading to cancer cell apoptosis [7]. Although carboplatin and oxaliplatin have a similar mechanism of action as cisplatin and exhibit some advantages over cisplatin, the drawback of dose-limiting toxicities and intrinsic or acquired resistance remain [8]. In order to reduce the side effects and overcome the resistance of cisplatin, it has been investigated on new platinum drugs with elevated antitumor efficiency and more tolerable toxicological profile [9].

[a.] Laboratorio de Nanobiomateriales, CINDEFI - Departamento de Química, Facultad de Ciencias Exactas, Universidad Nacional de La Plata-CONICET (CCT La Plata), Calle 47 y 115, B1900AJL La Plata, Argentina.
[b.] Laboratorio de Investigación y Desarrollo de Bioactivos (LIDeB), Departamento de Ciencias Biológicas, Facultad de Ciencias Exactas, Universidad Nacional de La Plata (UNLP), Calle 47 y 115, B1900AJI, La Plata, Buenos Aires, Argentina
[c.] Materiales Compuestos Termoplásticos (CoMP), Instituto de Investigaciones en Ciencia y Tecnología de Materiales (INTEMA), CONICET-Universidad Nacional de Mar del Plata (UNMdP). Av. Colón 10850, Mar del Plata 7600, Argentina.
[d.] Centro de Química Inorgánica, CEQUINOR (CONICET-UNLP), Bv 120 1465, La Plata, Argentina
† Footnotes relating to the title and/or authors should appear here.
Electronic Supplementary Information (ESI) available: [details of any supplementary information available should be included here]. See DOI: 10.1039/x0xx00000x

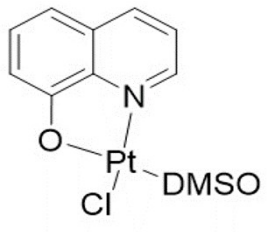

Figure 1: Chemical structure of [PtCl(8-O-quinoline)(dmso)] (8HQ-Pt) compound

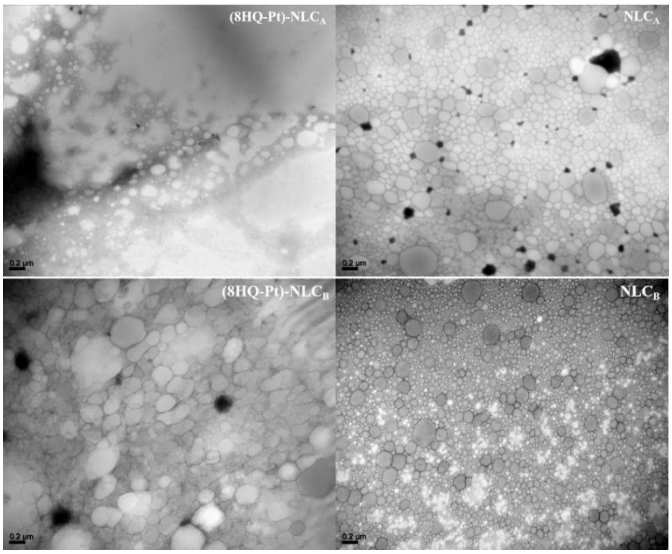

Figure 2: TEM images of NLCs; 8HQ-Pt compound loaded (left), empty (right).

Clioquinol has been used for medical applications such as the treatment of Alzheimer's disease because it is able to interact with metals like zinc or copper [10]. Clioquinol interaction of metals with DNA causes high cytotoxicity and induces apoptosis of cancer cells [11]. The drug 8-hydroxyquinoline platinum(II) **[PtCl(8-O-quinoline)(dmso)]** (8HQ-Pt) (**Figure 1**) was derived from clioquinol and showed antitumor activity without generating resistance and side effects up today when it is compared with cisplatin [12].

Nanosystems were developed to reduce and eliminate some disadvantages of many drugs with administration problems like cancer drugs, for instance, dosage-related side effects, drug resistance and poor aqueous solubility. These systems may provide improved drug performance by controlled release, i.e. preventing sudden increases in blood levels and leading to a decrease in the side effects of the active substance [13]. Furthermore, the use of non-toxic lipids without organic solvents in the synthesis ensures biocompatible, biodegradable and non-irritating nanoparticles [14,15].

Among nanosystems, nanostructured lipid carriers (NLC) are one of the most promising carriers for drug delivery. NLCs are second-generation solid lipid nanoparticles that consist of a mix of solid and liquid lipids stabilized with a biocompatible active compound [16]. NLCs were developed to overcome some drawbacks of solid lipid nanoparticles (SLN), such as drug instability and low drug loading capacity [17]. NLCs have a high capacity to load drugs and increase the solubility of drugs, especially hydrophobic molecules [18].

The current study aims to improve the availability of the **[PtCl(8-O-quinoline)(dmso)]** under physiological environments by an efficient encapsulation in presence of two different types of liquid oils: capric triglyceride and olive oil, in order to achieve a sustained drug release profile and enhanced antitumor effects. Drug encapsulation efficiency, cytotoxicity, cell uptake and apoptosis analysis of nanoparticles were performed. Physicochemical characterization of the formulations was carried out by dynamic light scattering (DLS), transmission electron microscopy (TEM), Fourier transformed infrared spectroscopy (FTIR), thermogravimetric analysis (TGA), differential scanning calorimetry (DSC) and X-ray diffraction (XRD).

Results and discussion

Formulation development and nanoparticle morphology

All the formulations were produced with the same type and amount of solid lipid and surfactant, changing only the liquid oil (NLC$_A$: capric triglyceride, NLC$_B$: olive oil). For both 8HQ-Pt compound loaded formulations, the initial amount of drug was constant, and the encapsulation efficiency were 82.1 ± 0.9 and 81.5 ± 3.72 for (8HQ-Pt)-NLC$_A$ (8HQ-Pt)-NLC$_B$, respectively.

The morphological structure and size distribution of nanoparticles were analyzed by TEM (**Figure 2**). Both NLC systems exhibited spherical morphology and the size of both formulations are smaller than 200 nm. TEM images revealed the size of NLC$_A$ was smaller than NLC$_B$. These results were confirmed by DLS analysis.

The mean particle size and polydispersity index (PdI) of the formulations were determined by DLS. The average (± sd) particle size of NLC$_A$, (8HQ-Pt)-NLC$_A$, NLC$_B$ and (8HQ-Pt)-NLC$_B$ were 136.0 ± 1.1, 136.3 ± 0.5, 159.0 ± 2.0 and 144.0 ± 2.0 nm respectively (Table 1). The PdI values for all the formulations were determined around 0.2 which indicates monodisperse particle sizes [19].

Table 1: Average size and P_{dI} of NLCs by DLS. No significant differences were found among formulations (ANOVA, p>0.05). Z_{av} - Average size (nm), P_{dI} – Polydispersity index.

Formulations	Z_{av} (nm)	P_{dI}
NLC$_A$	136.0 ± 1.1	0.218 ± 0.016
NLC$_B$	159.0 ± 2.0	0.226 ± 0.010
(8HQ-Pt)-NLC$_A$	136.3 ± 0.5	0.218 ± 0.050
(8HQ-Pt)-NLC$_B$	144.0 ± 2.0	0.210 ± 0.013

Physicochemical characterization by FTIR, TGA, DSC and XRD analysis

FTIR analysis was performed to identify the surface functional groups and their interaction with the matrix. Cetyl esters (SS) showed characteristic peaks in the range of 2915 cm^{-1} and 2847 cm^{-1} (alkane C-H stretching) and 1731 cm^{-1} (aldehyde C=O stretching). These peaks were observed in the spectra of NLC$_A$, (8HQ-Pt)-NLC-A, NLC$_B$ and (8HQ-Pt)-NLC$_B$ nanoparticles (**Figure 3**) [20].

The FTIR spectra of surfactant Poloxamer 188 showed characteristic peaks of the alkane group (C-H peak at 2873 cm^{-1}), the alcohol group (O-H stretching peak at 1340 cm$^{-1)}$ and the secondary alcohol group (C-O stretching peak at 1096 cm^{-1}) [21].

The liquid oil capric triglyceride that was incorporated in the formulations NLC$_A$ and (8HQ-Pt)-NLC$_A$ showed absorption bands at 2923 cm^{-1}, 1739 cm^{-1} and 1148 cm^{-1} which are related with alkane C-H stretching, aldehyde C=O stretching and aliphatic ether C-O stretching, respectively. Olive oil contained in the formulations NLC$_B$ and (8HQ-Pt)-NLC$_B$ exhibited some peaks at 2923 cm^{-1} (alkane C-H stretching), 1741 cm^{-1} (esters C=O stretching) and 1160 cm^{-1} (tertiary alcohol C-O stretching) [22,23].

TGA and DSC analysis were used to analyze the thermal characteristics of the nanoparticles. According to the TGA results, NLC$_A$, (8HQ-Pt)-NLC$_A$, NLC$_B$ and (8HQ-Pt)-NLC$_B$ exhibited a biphasic thermal behavior. The first thermal degradations appeared in the range of 186-338 ºC with a weight loss of 37.3%, 33.9%, 33.2% and

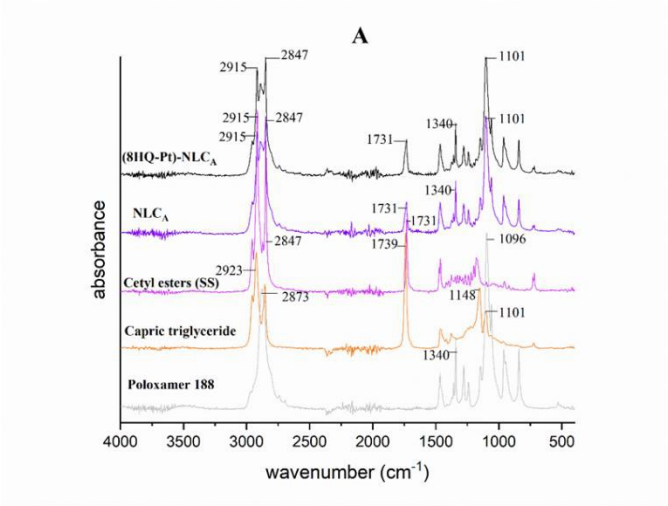

Figure 3: FTIR spectra of Cetyl esters (SS), Poloxamer 188, liquid oils; capric triglyceride and olive oil and NLC$_A$, (8HQ-Pt)-NLC$_A$, NLC$_B$ and (8HQ-Pt)-NLC$_B$ nanoparticles.

30.3%, respectively and are related to the cetyl esters (SS). All the formulations preserved their consistencies up to 185 ºC. That allows the NLCs to endure in release media. The second thermal degradations appeared in the range of 338 – 421 ºC with a weight loss of 62.5%, 65.9%, 66.0% and 68.7% respectively. TGA graph showed that NLC$_B$ formulations were more stable than NLC$_A$ formulations (**Figure SM1**). This fact can be attributed to the presence of high content of unsaturated fatty acids (*i.e.* about 85%) in olive oil in the NLC$_B$ formulation allowed to interact better with the drug [23].

DSC curves of the free 8HQ-Pt compound, NLC$_A$, (8HQ-Pt)-NLC$_A$, NLC$_B$, (8HQ-Pt)-NLC$_B$, cetyl esters (SS) and Poloxamer 188 were shown in Figure SM2. All formulations displayed two endothermic peaks. The first peaks were observed in the range of 44 – 48 ºC and it can be attributed to the melting point temperature of solid lipid cetyl esters (SS) which is approximately 44 ºC [15]. The second peaks were observed in the range of 46 – 52 ºC that could be associated with the melting point temperature of Poloxamer 188 (approximately 53 ºC). The free 8HQ-Pt compound did not show degradation up to 100 ºC which indicates its good stability under the operational conditions.

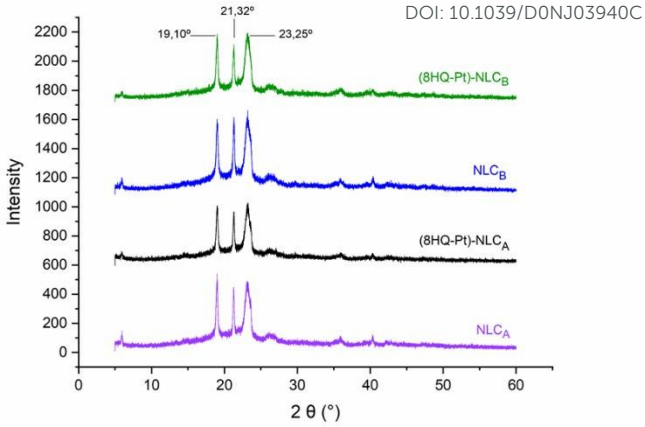

Figure 4: XRD patterns of empty and loaded NLC nanoparticles

Crystalline structures of the NLCs with or without 8HQ-Pt compound (NLC$_A$, (8HQ-Pt)-NLC$_A$, NLC$_B$ and (8HQ-Pt)-NLC$_B$ were analyzed by XRD to identify the polymorphism of the lipid matrix. Fats can crystalize in α (unstable), β' (metastable) and β (stable) polymorphic forms [24]. The assignment of XRD peaks indicates a mixture of β and β' forms of the lipids. All the NLC formulations showed comparable patterns. The patterns equivalent to NLC formulations displayed peaks correlative to cetyl esters SS (19.10°, 21.32° and 23.25°) and confirm the solid crystalline structure of NLCs (**Figure 4**) [15]. Short spacing (d) of crystal lattices is utilized to characterize the polymorphic forms. NLC formulations exhibited short spacing at 0.46 nm (β form), 0.42 nm (β' from) and 0.38 nm (β or β' form) where the peaks were observed at 19.10°, 21.32° and 23.25°, respectively [25]. Polymorphic behavior due to the crystalline structure of lipid nanoparticles is crucial for stability during storage and the release properties of the loaded drug from the nanoparticles. β or β' forms display higher-order packing and highest thermodynamic stability. Thus, undesirable drug expulsions could be prevented [20,26].

In vitro drug release assay

In vitro drug release assay was performed at pH 4.4 in 200 mM acetate buffer by the dialysis method. 2.0 mL of each formulation as well as a free-drug suspension were placed into dialysis bags and the release profiles were analyzed (**Figure 5**). Free 8HQ-Pt reached 100% release in the first 3 h. In comparison with free 8HQ-Pt compound suspension, both formulations displayed slow drug release rate, with approximately 75% (8HQ-Pt)-NLC$_A$ and 90% (8HQ-Pt)-NLC$_B$ released in 72 h. Figure 5 showed hyperbolic curves for 8HQ-Pt compound release kinetic from the nanoparticles. When studying the drug release from the nanoparticles, it was found that the date better

View Article Online
DOI: 10.1039/D0NJ03940C

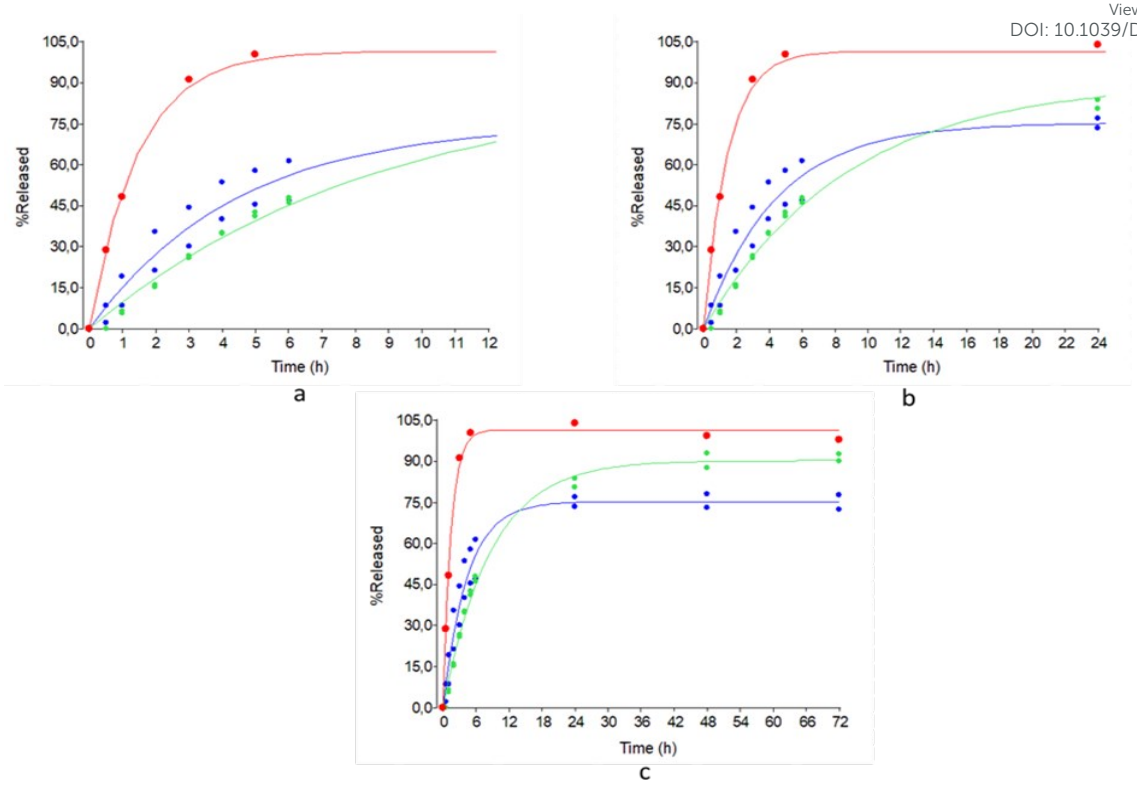

Figure 5: Release profiles (Mean ± SD) of (8HQ-Pt)-NLC$_A$ (blue), (8HQ-Pt)-NLC$_B$ (green) nanoparticles and free 8HQ-Pt compound (red) during 12 h (a), 24 h (b) and 72 h (c).

adjust to a first-order release kinetic [27]. (*Eq. 1*), according to all the statistical goodness of fit measures considers (R^2, R^2-adj, AIC, MSE and residual structure).

$$F_t = \frac{M_t}{M_\infty} \times 100 = F_{max}\left(1 - e^{-k \cdot t}\right) \qquad Eq.\ 1$$

In the equation, F_t is the percentage released at time t, M_t and M_∞ are the cumulative amounts of the compound released at time t and infinite time, respectively; F_{max} and k are the parameters to be estimated, also known as the scale and shape parameters, respectively. The results of the modelling analysis are shown in Table SM1, along with some goodness of fit measures.

A first-order kinetic means that the device releases the drug in a way that is proportional to the amount of drug remaining in its interior. Despite that is difficult to conceptualize this model in a theoretical basis [28], it is informative to compare the value of the kinetic constant k (scale parameter) among the formulations since it contains the information about the influence of the formulation on the drug release. As it can be seen in Table SM1, while the free 8HQ-Pt compound on the dialysis bag shows a k=0.7, the nanoparticles possess values of 0.23 and 0.12 (for NLC$_A$ and NLC$_B$, respectively). In other words, the nanoparticles were able to control the release speed by decreasing the kinetic constant more than a half, in comparison with the free 8HQ-Pt compound.

Cytotoxicity assay

The human intestinal cell line HT-29 was isolated from colon adenocarcinoma cells [29]. 95% of colorectal tumors are adenocarcinoma which becomes malignant from epithelial cells of the colorectal mucosa and related with the glands [30]. HT-29 cell line is one of the most used *in vitro* models in the anticancer studies. It is reported that HT-29 cell line showed resistance to chemotherapy drugs [31,32]. model to clarify the mechanism of acquired resistance in preclinic cancer investigations 33.

Cell cytotoxicity assay was performed for NLCs and free 8HQ-Pt compound on HT-29 colon carcinoma cell line by MTT analysis (Figure 6). Cells were treated with 5, 10 and 25 µM concentration of 8HQ-Pt compound for 24 h. The results showed that unloaded NLCs were non-toxic while (8HQ-Pt)-NLC$_A$ and (8HQ-Pt)-NLC$_B$ showed a cytotoxic effect in HT-29 cells correlated with drug concentration. The cell viability values dropped to 45.0% (free drug), 44.4% ((8HQ-Pt)-NLC$_A$), 78.5% ((8HQ-Pt)-NLC$_B$) for 5 µM, 12.0%, 17.9%, 54.4% for 10 µM and 11.0%, 10.1%, 16.5% for 25 µM, respectively. Moreover, the type of liquid oil has a different effect on cell viability. (8HQ-Pt)-NLC$_A$ synthesized with capric triglyceride exhibited more cytotoxicity than (8HQ-Pt)-NLC$_B$ synthesized with olive oil but showed similar cytotoxic effect with the free 8HQ-Pt compound. This result can be attributed to 8HQ-Pt compound was released in a time-dependent controlled manner from the nanoparticle in 24 h. On Figure 5 is displayed that the release of 8HQ-Pt from NLC$_A$ and NLC$_b$ roughly is 75% compared to 100% of free drug so which means that 8HQ-Pt-NLC$_A$ is possess approximately 25% more cytotoxic effect than the free drug. This advantage could be significant considering a potential

iv administration in where the injected formulation is circulating in the blood flow to reduce undesirable secondary effects.

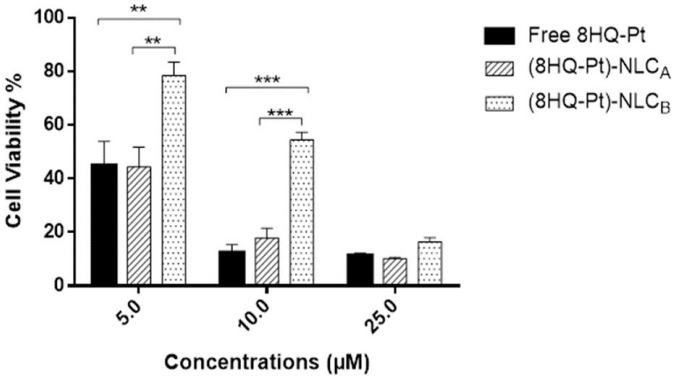

Figure 6: Cell cytotoxicity 8HQ-Pt loaded NLC formulations in HT-29 cell line. Concentration-dependent cytotoxicity of free 8HQ-Pt compound and 8HQ-Pt loaded NLCs in HT-29 cells for 24 h.

Cellular uptake of NLCs

Cellular uptake of NLCs into HT-29 cells was performed to evaluate the internalization of the nanoparticles. Firstly, the NLCs were labelled with fluorescent probe DiOC18 and then, the cells were incubated with the empty labelled nanoparticles using three different concentrations of NLCs (equivalent amount for 5, 10 and 25 μM (8HQ-Pt)-NLCs for 6 h. Subsequently, the fluorescent signals were followed by flow cytometry. It was observed that the cellular uptake of NLCs increased directly correlated with their concentrations. Furthermore, the results showed that NLC_A was more capable to penetrate to the HT-29 cells than NLC_B (Table 2). This data confirmed the cytotoxicity assay result. Neves et al. compared cellular uptake properties of NLC and SLN and emphasized that NLCs exhibited higher internalization to the colon carcinoma cells due to the presence of liquid oil [34].

Table 2: Cell uptake of DiOC18-loaded cetyl esters (SS) NLCs in HT-29. Flow cytometry was utilized to detect the cell uptake of labelled NLCs. The cells were incubated for 6 h at the concentrations that equivalent amount for 5, 10 and 25 μM Pt-NLCs.

Concentration (μM)	NLC_A	NLC_B
5	54.7	22.5
10	72.1	30.7
25	88.1	55.0

In addition to the presence of liquid oil, our study also revealed the importance of the type of liquid oil. The NLCs with capric triglyceride achieved more cellular uptake efficiency than the NLCs with olive oil. Safwat *et al*. analyzed the effect of 3 types of liquid oils (Labrafil®, Labrasol® and Labrafac lipophile®) to the antitumor activity of NLC. Simvastatin loaded NLCs with Labrasol® showed the highest cellular uptake and cytotoxic effect on MCF-7 cancer cells [35]. Lan et al. reported that lipid-coated cisplatin showed enhanced cellular uptake in CAL 27, SCC 15 and FaDu cancer cell lines when compared with free cisplatin [36].

Apoptosis

Antitumor drugs have effectiveness to prevent cell proliferation and generate cell apoptosis. During apoptosis process, phosphatidylserine residues translocate to the outer of the cell membrane. Annexin V–FITC is a fluorescent dye that binds to phosphatidylserine receptor. Thus, the apoptotic cells become detectable by fluorescence assays [37].

HT-29 cells were stained with Annexin V–FITC/PI apoptosis detection kit after 48 h treatment. Antitumor activity of the free 8HQ-Pt compound and (8HQ-Pt)-NLC_A were confirmed by flow cytometry. **Figure 7** shows the percentage of vital (V-/PI-), the early apoptotic (V+/PI-), the late apoptotic (V+/PI+) and the necrotic (V-/PI+) subpopulations in the dot plot. The results demonstrated that free 8HQ-Pt compound and (8HQ-Pt)-NLC_A induced 13.0% and 12.6% for 1.0 μM, 53.8% and 33.3% for 2.5 μM, 71.4% and 70.3% of cells in late apoptosis (V+/PI+), respectively. These results confirmed the cell viability assays that the late apoptotic cells values increased in a concentration-dependent manner in cells treated with free 8HQ-Pt compound and (8HQ-Pt)-NLC_A. On the other hand, empty nanoparticles exhibited very low apoptosis level. Ruiz *et al*. reported the antiproliferative effect of 8HQ-Pt by measuring mitochondrial transmembrane potential. They also proved that its apoptotic effect is in a concentration-depended manner in the MG-63 cell line [12]. Platinum-based drugs show limited plasma stability and low delivery, although their apoptotic effects [38]. Drug stability is increased by nanoencapsulation due to the interaction of the drug with the lipid [18]. Cacicedo *et al*. demonstrated that the antitumor activity of Metvan was enhanced by NLC encapsulation. This result was attributed to the drug protection property of NLC and therefore, higher drug accumulation occurred in the tumor cells and caused more apoptosis [39]. Thus, NLCs are encouraging nanosystems to overcome the problems of antitumor drugs and improve their therapeutic activities.

Experimental

Materials

Cetyl esters (SS) and capric triglyceride lipids were kindly donated by Croda (Argentina). Poloxamer 188 and 3,3'-dioctadecyloxacarbocyanine perchlorate (DiOC18) were purchased from Sigma–Aldrich (Buenos Aires, Argentina). DMEM (Dulbecco's Modified Eagles Medium) and TrypLE™ were purchased from Gibco (Gaithersburg, MD, USA), and FBS (fetal bovine serum) was bought from *Internegocios* S.A. (Argentina). Annexin V, Fluorescein isothiocyanate (FITC)/PI and tetrazolium salt MTT (3-(4,5-dimethylthiazol-2-yl)-2,5-diphenyl-tetrazolium-bromide) from Invitrogen Co. (Buenos Aires, Argentina). Other reagents were of analytical grade from available commercial sources and used as received from Merck (Darmstadt, Germany) or similar brand.

View Article Online DOI: 10.1039/D0NJ03940C

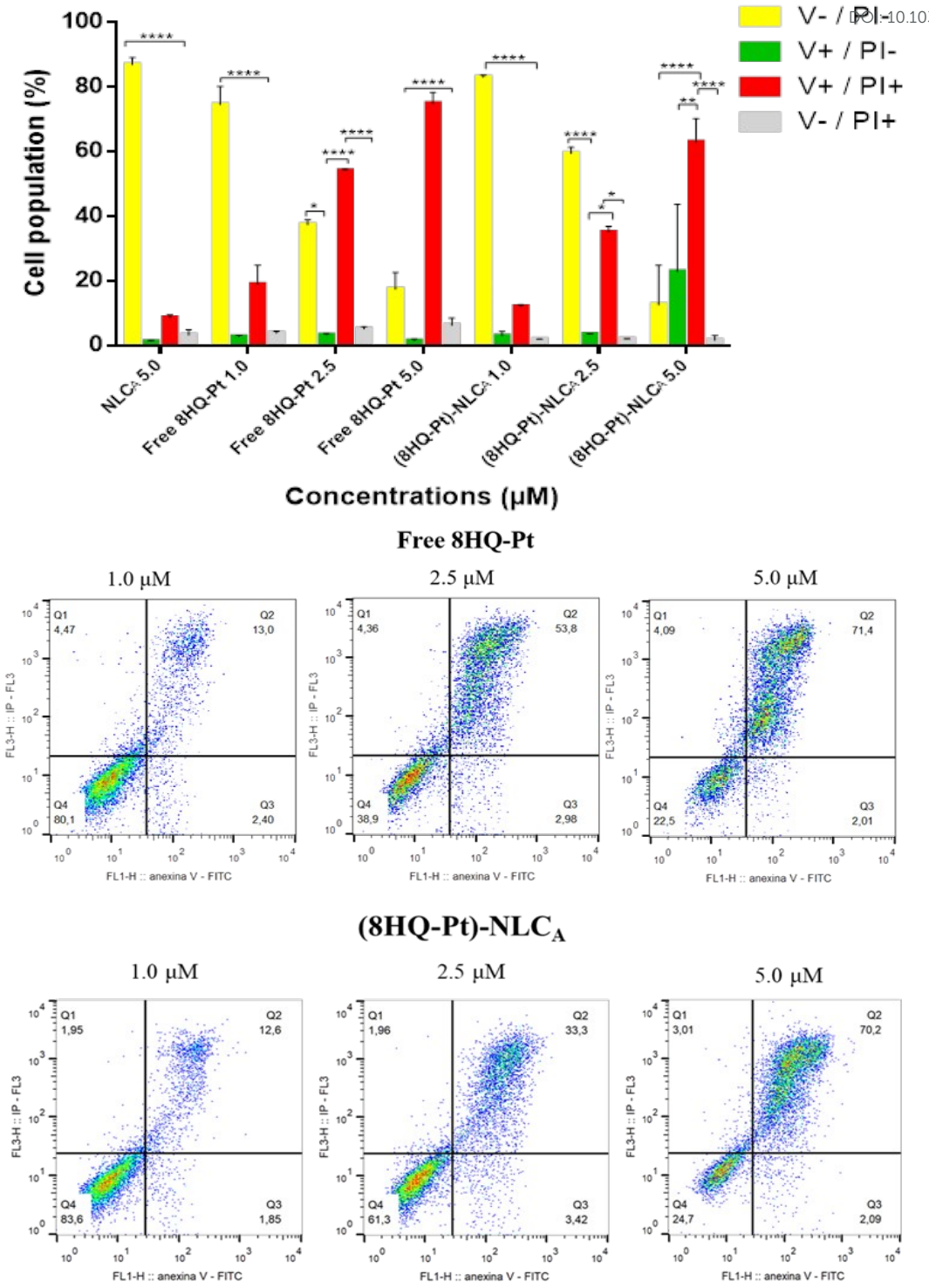

Figure 7: Apoptotic effects of free 8HQ-Pt compound and (8HQ-Pt)-NLC$_A$ at 1.0 μM, 2.5 μM and 5.0 μM after 48 h incubation with HT-29 cells.

Preparation of 8HQ-Pt compound

The **[PtCl(8-O-quinoline)(dmso)]** was synthesized and characterized according to Martín Santos C, *et al*. [11]. The product was obtained following the general procedure as a yellow-orange solid (78% yield) without further purification.

1H NMR (300 MHz, CD2Cl2) δ 9.41 (dd, J = 10.7, 1.2 Hz, 1H), 8.38 (dd, J = 8.4, 1.1 Hz, 1H), 7.58-7.40 (m, 2H), 7.02-7.06 (m, 2H), 3.61 (s, 6H). **13C NMR (75 MHz, CD2Cl2)** δ 148.6, 148.3, 140.3, 140.2, 131.5, 131.0, 121.7, 115.6, 114.6. 46.6. **195Pt NMR (64.5 MHz, CD2Cl2)** δ: -2760.7. **HRMS (FAB+):** calcd for $C_{11}H_{12}ClNO_2PtS$ (M+): 452.9915; found: 452.9928. **Anal. calcd**. for $C_{11}H_{12}ClNO_2PtS$: C, 29.18; H, 2.67; N, 3.09; found: C, 29.00; H, 2.67; N, 2.94.

Preparation of 8HQ-Pt compound loaded NLCs

[PtCl(8-O-quinoline)(dmso)] compound loaded NLCs were prepared by ultrasonication technique [20,40]. Briefly, 400 mg of solid lipid cetyl esters (SS) (2.0%, w/v) was melted in a water bath at 70 °C and mixed with 2.0 mg of the 8HQ-Pt compound. **[PtCl(8-O-quinoline)(dmso)]** was dissolved in 200 µL capric triglyceride or olive oil (1.0%, v/v). After 15 min, 20 mL of the hot aqueous solution of Poloxamer 188 (4.5%, w/v) was added to the lipid phase. Instantly, the mixture was ultrasonicated at 65% amplitude for 30 min equipped with 6 mm titanium tip (ultrasonic processor Cole Parmer, USA, 130 Watts). After sonication, the formulation was cooled down at room temperature and stored at 4 °C. Two different groups of lipid formulations were synthesized. The first group contained capric triglyceride: (8HQ-Pt)-NLC_A and its control NLC_A without the drug. The second one was similarly prepared and contained olive oil (74% oleic acid, 13% palmitic acid and small amount other fatty acids): (8HQ-Pt)-NLC_B and its control NLC_B.

Measurement of encapsulation efficiency

Encapsulation efficiency (EE, %) was calculated by measuring the concentration of the free drug in solution. Briefly, 500 µL of final suspension was transferred to an ultrafiltration centrifugal device (MWCO 10.000, Microcon®, Millipore, MA, USA) and centrifuged at 12000 ×g for 30 min. After centrifugation, the supernatant containing the free drug was measured by HPLC. The EEs (%) of the NLCs were estimated following equation 2 (*Eq. 2*):

$$EE\ (\%) = (w_i - w_{fd}) / w_i \times 100 \qquad Eq.\ 2$$

where w_i is the initial amount of Pt compound added to the formulation and w_{fd} is the amount of free Pt compound after the ultrafiltration process.

HPLC analysis of Pt compound

Chromatographic analysis was performed using HPLC (Gilson SAS, Villiers-Le-Bel, France) with UV detection. Chromatographic separation was performed in a Lichrosphere® 100 RP-18 (250 mm x 4.6 mm, 5 µm, Merck KGaA, Darmstadt, Germany) column. The mobile phase was methanol and 0.1% phosphoric acid solution (60:40). The system was operated isocratically at 1.0 ml/min flow rate and the detection was performed at 262 nm. Samples were diluted with mobile phase and centrifuged (15.000 x*g* for 5 min at 4 °C) prior to their injection (20 µL).

The method was validated in terms of linearity, precision, and specificity, over the range of expected concentrations (0.1 – 200 µM). Linear regression for the Pt compound ($p < 0.0001$) was observed in the concentration range of 0.2 – 110 µM, with a coefficient of determination R^2 = 0.997. The 95% confidence interval of the intercept was [-1.2322 – 0.6447]. The precision of the method was established at three concentration levels: 0.2, 44 and 110 µM, and in all cases RSD values were below 3%. The method was specific for 8HQ-Pt compound and no interfering peaks were observed.

Particle size and polydispersity index (PdI)

The average diameter and size distribution of lipid nanoparticles were measured by dynamic light scattering (DLS) (Nano ZS Zetasizer, Malvern Instruments Corp, UK) at 25 °C in polystyrene cuvettes with a thickness of 10 mm. Measurements were performed in 10 mm path length capillary cells, using deionized water (Milli-Q®, Millipore, Ma., USA). The PdI value was also determined. All the measurements were carried out in triplicate.

Transmission electron microscopy (TEM)

TEM analysis was performed using Jeol-1200 EX II-TEM microscope (Jeol, MA, USA). The NLC dispersion was 1:10 diluted with ultra-pure Milli-Q® water, and 10 µL of the dispersion was spread onto a collodion-coated Cu grid (400-mesh). Liquid excess was removed with filter paper and for contrast enhancement a drop of phosphotungstic acid as added to the NLCs dispersion.

Fourier transformed infrared spectroscopy (FTIR)

Fourier transform infrared spectroscopy (FTIR) was performed by using a Nicolet 6700 (Thermo Scientific, Inc., Waltham, MA, USA) spectrometer. Attenuated total reflectance (ATR) mode was used to record spectra over the range 600 – 4.000 cm^{-1} are the solution of 2 cm^{-1}.

Thermogravimetric analysis (TGA)

TGA was achieved with the aim to analyze the thermal stability of cetyl esters (SS), free (8HQ-Pt) compound, NLC_A, (8HQ-Pt)-NLC_A, NLC_B, (8HQ-Pt)-NLC_B particles. TGA Q500 apparatus (TA Instruments, New Castle, DE, USA) was used to obtain TGA data. Samples of 2.0 - 9.0 mg were accurately weighed in a platinum pan and measurements conducted from room temperature to 600 ºC at a heating rate of 10 ºC/min under nitrogen atmosphere to avoid the thermo-oxidative oxidation.

Differential Scanning Calorimetry (DSC) analysis

The thermal properties of cetyl esters (SS), free (8HQ-Pt) compound, NLC_A, (8HQ-Pt)-NLC_A, NLC_B, (8HQ-Pt)-NLC_B particles were determined by differential scanning calorimetry (DSC Q5000, TA Instruments, USA) under nitrogen atmosphere. Scans were run at 0 to 200°C range with heating rate of 10°C/min.

X-ray diffraction (XRD)

The X-ray diffraction patterns were obtained with a PANalytical X'Pert PRO diffractometer equipped with an X-ray source (Phillips PW 1830, PANalytical BV, the Netherlands) using CuKα radiation at 40 kV and 40 mA, over a 2θ range of 5° – 60° with an acquisition time of 1s/s at each step of 0.02°.

In vitro drug release assay

Release assays were performed using dialysis membranes (MWCO 10 kDa). The membrane was soaked in distilled water for overnight and filled with 2.0 ml of each formulation followed by immersion in 15.0 mL of 200 mM acetate buffer (pH = 4.4) at 37 ºC, with continuous shaking at 200 rpm. Samples of 200 µL were withdrawn at regular intervals for 72 hours, and drug concentration was measured in HPLC.

Cell cytotoxicity assay

HT-29 (human colon carcinoma cells) cell line was obtained from ATCC® (HTB-38™). Cells were cultured in Dulbecco's modified Eagle's medium (DMEM; Gibco, Invitrogen Corporation, USA) supplemented with 10% FBS (*Internegocios*, Buenos Aires, Argentina) and antibiotics (100 U/ml penicillin and 100 µg/ml streptomycin; Gibco, Invitrogen Corporation, USA) at 37ºC and under 5% CO_2 atmosphere. Cell viability was examined by the 3-(4,5-dimethylthiazol-2-yl)-2,5-diphenyltetrazolium bromide (MTT) [41]. HT-29 cells were seeded in a 96-well plate for 24 h to be attached to the plate surface. Then, the cells were treated with different concentrations of free (8HQ-Pt) compound, NLC_A, (8HQ-Pt)-NLC_A, NLC_B, (8HQ-Pt)-NLC_B particles in serum-free DMEM for 24 h. The medium was removed, and the cells were incubated with MTT reagent (0.5 mg/mL MTT in supplemented DMEM medium) for 3 h. Later, the absorbance was read at 570 nm in a microplate reader (multiplate reader multiskan FC, thermo scientific). Cell viability was indicated as the percentage (%) of the untreated control value (100% survival).

Cellular uptake assay

Cellular uptake was evaluated using empty nanoparticles labelled with the green fluorescent probe DiOC18 ($\lambda_{abs}/\lambda_{em}$= 484/501 nm). Concisely, 1.0 mg of DiOC18 was mixed with the melted lipid phase (at 70 °C) and protected from light. The formulation was prepared as previously described by the addition of aqueous phase and sonication at 65% potency for 30 min. As a result, the DiOC18 was 100% encapsulated into the nanoparticles. The cellular uptake of fluorescent-labelled nanoparticles was evaluated by flow cytometry. HT-29 cells were plated in 12 well plate at the density of 20 ×10^4 cells per well. After 24 h, cells were treated with serum-free DMEM containing three different concentrations of empty NLCs (equivalent amount for 5, 10 and 25 µM (8HQ-Pt)-NLCs and incubated for 6 h. At the end of the treatment, cells were washed once with PBS. Then, cells were treated with 300 µL of trypLe and next, 600 µL of the serum-containing medium was added to each well. Later, cells were collected from each well to Eppendorf tubes and centrifuged at 2,500 ×g for 5 min. Supernatants were removed and cells were dispersed in 200 µL of PBS. Fluorescence was analyzed by FACSCalibur (Becton–Dickinson, Franklin Lakes, NJ, USA) and the resulting values were evaluated by FlowJo 7.6 software.

Apoptosis

Cells were treated with the three different concentrations (1.0, 2.5, 5.0 µM) and incubated for 48 h prior to analysis. For the staining, cells were washed with PBS and were diluted with 1X binding buffer, Annexin V-FITC and PI and incubated for 20 min at room temperature prior to analysis. Cells were collected using flow cytometry (BD FACSCalibur™) and the results were analyzed using FlowJo 7.6 software. Four subpopulations were defined in the dot plot: the undamaged vital (Annexin V−/PI−), the vital mechanically damaged (Annexin V/PI+), the early apoptotic (Annexin V+/PI−), and the late apoptotic (Annexin V+/PI+) subpopulations.

Statistical analysis

Experiments were carried out with a minimum of 3 independent replicas. Comparisons of the means were performed by analysis of variance (ANOVA) with a significance level of 5.0% (α= 0.05) followed by Fisher's least significant difference test.

Conclusions

In the present study, two novel, stable and smart NLC formulations were successfully synthesized by ultrasonication technique in the presence of capric triglyceride or olive oil: (8HQ-Pt)-NLCA and (8HQ-Pt)-NLCB.

According to TEM and DLS results that the nanoparticles displayed spherical shape and narrow size distribution with low *PdI* (lower than 0.25) which are indicatives of the incorporation of 8HQ-Pt compound into the NLCs. Besides, an efficient encapsulation higher than 80% were founded for both formulations In addition, the physicochemical characterization of the formulations by FTIR, TGA, DSC and XRD proved the thermal properties, surface composition and crystalline structures of the free 8HQ-Pt compound, loaded and empty formulations. Compared to the free drug, both nanoparticles showed a slower and more sustained release profile during 72 h, which guarantee the biodistribution of the nanoparticles as such, at the same time that they release their cargo. The cytotoxicity effect, cell uptake and apoptosis assays of 8HQ-Pt compound loaded nanostructured lipid carrier (NLC) formulations were evaluated in a dose-dependent manner on human colon adenocarcinoma cell line HT-29. (8HQ-Pt)-NLC_A showed similar effects with free 8HQ-Pt compound on HT-29 cells but without the deleterious effects of the free drug, and with enhanced biocide activity over cancer cells. Additionally, the nanosystems may provide other advantages over the free drug: protection from *in vivo* degradation, improved biodistribution profile and decreased undesirable side effects. Finally, our study suggests that 8HQ-Pt compound loaded NLCs could be a promising drug delivery system for colorectal cancer treatment with enhanced therapeutic efficacy.

Conflicts of interest

The authors declare that they have no conflict of interest to the publication of this article.

Acknowledgements

This work was supported by UNLP (X041, X701), CONICET (PIP 0340), and ANPCyT (PICT 2016-1574, PICT 2017-2251, PICT2016- 4597). IEL, MER, VAA and GRC are members of the Carrera del Investigador, CONICET, Argentina. TB and SSM have a CONICET fellowship, Argentina.

References

1 S. B. Wild CP, Weiderpass E, *World cancer report 2020*, 2020.

2 S. Schlesinger, K. Aleksandrova, L. Abar, A. R. Vieria, S. Vingeliene, E. Polemiti, C. A. T. Stevens, D. C. Greenwood, D. S. M. Chan, D. Aune and T. Norat, *Ann. Oncol.*, 2017, **28**, 1217–1229.

3 L. Kelland, *Nat. Rev. Cancer*, 2007, **7**, 573–584.
4 X. Chen, Y. Wu, H. Dong, C. Zhang and Y. Zhang, *Curr. Mol. Med.*, 2013, **13**, 1603–1612.
5 L. Galluzzi, L. Senovilla, I. Vitale, J. Michels, I. Martins, O. Kepp, M. Castedo and G. Kroemer, *Oncogene*, 2012, **31**, 1869–1883.
6 W. A. Wani, S. Prashar, S. Shreaz and S. Gómez-Ruiz, *Coord. Chem. Rev.*, 2016, **312**, 67–98.
7 S. Dasari and P. Bernard Tchounwou, *Eur. J. Pharmacol.*, 2014, **740**, 364–378.
8 B. W. Harper, A. M. Krause-Heuer, M. P. Grant, M. Manohar, K. B. Garbutcheon-Singh and J. R. Aldrich-Wright, *Chem. - A Eur. J.*, 2010, **16**, 7064–7077.
9 X. Wang and Z. Guo, *Chem. Soc. Rev.*, 2013, **42**, 202–224.
10 A. D. Schimmer, *Curr. Cancer Drug Targets*, 2011, **11**, 325–331.
11 C. Martín Santos, S. Cabrera, C. Ríos-Luci, J. M. Padrón, I. López Solera, A. G. Quiroga, M. A. Medrano, C. Navarro-Ranninger and J. Alemán, *Dalt. Trans.*, 2013, **42**, 13343.
12 M. C. Ruiz, A. Resasco, A. L. Di Virgilio, M. Ayala, I. Cavaco, S. Cabrera, J. Aleman and I. E. León, *Cancer Chemother. Pharmacol.*, 2019, **83**, 681–692.
13 M. Sato, P. da Silva, R. de Souza, K. dos Santos and M. Chorilli, *Curr. Top. Med. Chem.*, 2015, **15**, 287–297.
14 M. A. Iqbal, S. Md, J. K. Sahni, S. Baboota, S. Dang and J. Ali, *J. Drug Target.*, 2012, **20**, 813–830.
15 S. Scioli Montoto, M. L. Sbaraglini, A. Talevi, M. Couyoupetrou, M. Di Ianni, G. O. Pesce, V. A. Alvarez, L. E. Bruno-Blanch, G. R. Castro, M. E. Ruiz and G. A. Islan, *Colloids Surfaces B Biointerfaces*, 2018, **167**, 73–81.
16 G. A. Islan, M. L. Cacicedo, B. Rodenak-Kladniew, N. Duran and G. R. Castro, *Curr. Pharm. Des.*, 2018, **23**, 6643–6658.
17 Q. Li, T. Cai, Y. Huang, X. Xia, S. Cole and Y. Cai, *Nanomaterials*, 2017, **7**, 122.
18 A. Puri, K. Loomis, B. Smith, J. Lee, A. Yavlovich, E. Heldman and R. Blumenthal, *Crit. Rev. Ther. Drug Carr. Syst.*, 2009, **26**, 523–580.
19 W. Schärtl, *Light Scattering from Polymer Solutions and Nanoparticle Dispersions*, Springer Berlin Heidelberg, Berlin, Heidelberg, 2007.
20 B. Rodenak-Kladniew, G. A. Islan, M. G. de Bravo, N. Durán and G. R. Castro, *Colloids Surfaces B Biointerfaces*, 2017, **154**, 123–132.
21 F. Yan, C. Zhang, Y. Zheng, L. Mei, L. Tang, C. Song, H. Sun and L. Huang, *Nanomedicine Nanotechnology, Biol. Med.*, 2010, **6**, 170–178.
22 M. Pan, S. Sun, Q. Zhou and J. Chen, *J. Food Sci.*, 2018, **83**, 1605–1612.
23 M. Lei, F.-C. Jiang, J. Cai, S. Hu, R. Zhou, G. Liu, Y.-H. Wang, H.-B. Wang, J.-R. He and X.-G. Xiong, *Int. J. Biol. Macromol.*, 2018, **111**, 755–761.
24 D. Rousseau, A. G. Marangoni and K. R. Jeffrey, *JAOCS, J. Am. Oil Chem. Soc.*, 1998, **75**, 1833–1839.
25 E. ten Grotenhuis, G. A. van Aken, K. F. van Malssen and H. Schenk, *J. Am. Oil Chem. Soc.*, 1999, **76**, 1031–1039.
26 Y. Rosiaux, V. Jannin, S. Hughes and D. Marchaud, *J. Control. Release*, 2014, **188**, 18–30.
27 P. Costa and J. M. Sousa Lobo, *Eur. J. Pharm. Sci.*, 2001, **13**, 123–133.
28 M. L. Bruschi, *Strategies to Modify the Drug Release from Pharmaceutical Systems*, Elsevier, 2015.
29 J. Fogh and G. Trempe, in *Human Tumor Cells in Vitro*, Springer US, Boston, MA, 1975, pp. 115–159.
30 M. Fleming, S. Ravula, S. F. Tatishchev and H. L. Wang, *J. Gastrointest. Oncol.*, 2012, **3**, 153–73.
31 M. Mohammadian, S. Zeynali, A. Azarbaijani, M. Khadem Ansari and F. Kheradmand, *Res. Pharm. Sci.*, 2017, **12**, 517.
32 F. El Khoury, L. Corcos, S. Durand, B. Simon and C. Le Jossic-Corcos, *Int. J. Oncol.*, 2016, **49**, 2558–2568.
33 K. J. Gotink, H. J. Broxterman, R. J. Honeywell, H. Dekker, R. R. de Haas, K. M. Miles, R. Adelaiye, A. W. Griffioen, G. J. Peters, R. Pili and H. M. W. Verheul, *Oncoscience*, 2014, **1**, 844–853.
34 A. R. Neves, J. F. Queiroz, S. A. Costa Lima, F. Figueiredo, R. Fernandes and S. Reis, *J. Colloid Interface Sci.*, 2016, **463**, 258–265.
35 S. Safwat, R. A. H. Ishak, R. M. Hathout and N. D. Mortada, *Drug Dev. Ind. Pharm.*, 2017, **43**, 1112–1125.
36 X. Lan, J. She, D. Lin, Y. Xu, X. Li, W. Yang, V. W. Y. Lui, L. Jin, X. Xie and Y. Su, *ACS Appl. Mater. Interfaces*, 2018, **10**, 33060–33069.
37 M. Hassan, H. Watari, A. AbuAlmaaty, Y. Ohba and N. Sakuragi, *Biomed Res. Int.*, 2014, **2014**, 1–23.
38 S. Dilruba and G. V. Kalayda, *Cancer Chemother. Pharmacol.*, 2016, **77**, 1103–1124.
39 M. L. Cacicedo, M. C. Ruiz, S. Scioli-Montoto, M. E. Ruiz, M. A. Fernández, R. M. Torres-Sanchez, E. J. Baran, G. R. Castro and I. E. León, *New J. Chem.*, 2019, **43**, 17726–17734.
40 G. A. Islan, P. C. Tornello, G. A. Abraham, N. Duran and G. R. Castro, *Colloids Surfaces B Biointerfaces*, 2016, **143**, 168–176.
41 T. Mosmann, *J. Immunol. Methods*, 1983, **65**, 55–63.

View Article Online
DOI: 10.1039/D0NJ03940C

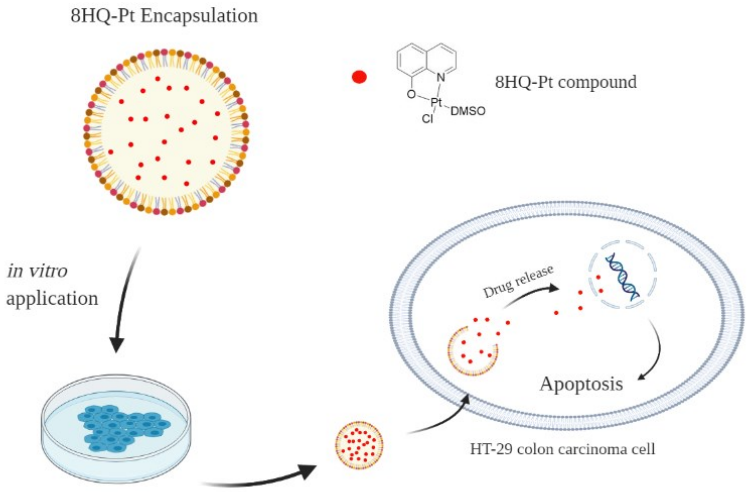

314x419mm (72 x 72 DPI)